Nanoscale Advances

COMMUNICATION

View Article Online
View Journal | View Issue

Cite this: *Nanoscale Adv.*, 2019, **1**, 1721

On-surface trapping of alkali atoms by crown ethers in ultra high vacuum†

Matus Stredansky, [ab] Elia Turco, [ab] Zhijing Feng, ‡[ab] Roberto Costantini, [ab] Giovanni Comelli, [ab] Alberto Verdini, [a] Luca Floreano, [a] Alberto Morgante, [ab] Carlo Dri §[ab] and Albano Cossaro *[a]

Received 6th March 2019
Accepted 2nd April 2019

DOI: 10.1039/c9na00144a

rsc.li/nanoscale-advances

Crown ethers, assembled into a regular 2D array *via* a chemical guest–host recognition process, have been successfully employed to trap sodium atoms on a surface, under ultra-high vacuum conditions.

Introduction

Since their discovery by Pedersen in 1967,[1,2] crown ethers have played a relevant role in supramolecular chemistry for their suitability in complexing metal atoms and in hosting guest molecules. Due to their versatility, it has been estimated that more than 10 000 differently sized, substituted or functionalized crown ether molecules have been synthesized.[3] In their most simple form as they were originally synthesized, crown molecules are cyclic oligomers of $n(-CH_2CH_2O-)$ units, where $n = 4, 5, 6$ correspond to the most stable configurations. The electron lone pairs localized on the oxygen atoms and pointing towards the centre of the crown give the molecules the Lewis basicity that characterizes their chemical behavior. Crown derivatives have been extensively used both in solution and in gas phase to recognize and trap metal ions[4] and small ionic molecules.[5–7] This affinity has promoted interesting applications in biology,[3] where crowns are successfully employed to preserve the activity of enzymes in non-aqueous environments[8–10] or to act as antimicrobial and prospective antitumoral agents.[11] In the design of gas sensors, the functionalization of metal organic frameworks with crowns, introduces a tunability of the gas sensing properties of the system, the selective affinity towards specific gases being dependent of the alkali atoms used to dope the ethers.[12] Self-assembled monolayers of crown derivatives have been formed and used on surfaces to trap metal ions but with both the growth and trapping process performed in solution.[13–15] In fact, despite their unique coordinating properties, crown ethers have been poorly or not at all exploited in solid state and in particular in systems grown under ultra-high vacuum (UHV) conditions, where they could represent a promising tool in the design of complex interfaces potentially relevant for organic-based devices. The lack of such studies can be ascribed to their poor self-assembly properties: we have recently shown that their high chemical reactivity and their low structural rigidity prevent the crown ethers from self-organizing in ordered films when deposited on surfaces under UHV,[16] rather leading to the formation of inhomogeneous assemblies of clusters. To overcome this problem, we found a growth protocol that yields an ordered 2D array of amino-terminated crown ethers, based on a chemical guest–host interaction between the functionalized ethers and a carboxylic organic template grown on the Au(111) surface.[16] However, no information about the chemistry of the crown molecules in this architecture is known. In particular, the critical issue to investigate is the complexing functionality of the molecules, in order to determine whether it is preserved or rather inhibited by the crown–template interactions. To this aim, in this work we explore the reactivity of the crowns upon their anchoring in the 2D array. In particular, by exposing the system to sodium atoms, we probe *in situ* the alkali-crown affinity, well known for systems in solution. Our findings, supported by both X-ray photoemission spectroscopy (XPS) and scanning tunneling microscopy (STM) imaging, demonstrate that Na atoms are preferentially trapped by the crowns, indeed. Only when these sites are saturated further Na atoms start interacting with the supporting template. To our knowledge, this study represents the first example of crown–metal coordination entirely obtained in vacuum and may open to a more systematic employment of crown ethers in the formation of smart organo-metallic complexes under UHV.

[a]CNR-IOM Laboratorio TASC, Basovizza SS-14, km 163.5, I-34012 Trieste, Italy. E-mail: cossaro@iom.cnr.it

[b]Dipartimento di Fisica, Università di Trieste, via A. Valerio 2, I-34127 Trieste, Italy

† Electronic supplementary information (ESI) available: STM pulse manipulation of the Na/crown/CTPP system. See DOI: 10.1039/c9na00144a

‡ Present address: Department of Chemical Engineering and Materials Science, University of California, Irvine, Irvine, California 92697, USA.

§ Present address: ELETTRA-Sincrotrone Trieste S.C.p.A., Area Science Park S.S. 14 Km 163.5, 34012 Trieste, Italy.

Results and discussion

The assembly of the 2D array of crown ethers, namely the 2-aminomethyl-15-crown-5 (AMC), was obtained following the protocol we described elsewhere.[16] Briefly, a monolayer of carboxylic tetraphenylporphyrin (CTPP) molecules is grown on the Au(111) surface. The resulting system is a regular 2D array of carboxylic centers, which is used as a template to anchor a layer of AMC, the growth being driven by the amino-carboxylic chemical affinity. The crown molecules assemble in 2D arrays as well and the coexistence of two different phases is observed, characterized by different AMC : CTPP population ratio, either 1 : 2 or 1 : 1. Fig. 1, adapted from Feng *et al.*,[16] reports a model of the two molecules and the STM image of the crown array in the 1 : 2 phase. The single AMC molecules are the bright, isolated and round-shaped features positioned between the CTPP molecules. The crown body of AMC consists of 5 oxygen and 10 carbon atoms. When employed in solution, this ether is known to have high affinity for sodium ions, due to the good size matching between crown and atoms.[4] In order to probe the chemical activity of the crown molecules in our anchored architecture we exposed the system to atomic Na flux and monitored both the chemistry and the morphology of the system by means of XPS and STM respectively. As a reference, first we deposited Na on top of the CTPP template. Fig. 2 reports the C 1s and N 1s XPS spectra of the template at increasing Na coverage as well as the STM image taken at an intermediate Na doping stage. The Na coverage in the XPS spectra is indicated in units of a reference value, θ_{Na}, previously determined by XPS analysis of the deposition of Na atoms on the Au(111) substrate as corresponding to 1 Na atom per 60 ± 10 Au atoms of the topmost layer and also, more conveniently, per CTPP molecule at the monolayer stage (see Materials and methods). Both C 1s and N 1s sequences of spectra are characterized by a shift of the peaks towards the high binding energies as the doping increases. In particular, in the N 1s spectra at $\theta_{Na} = 0$ two main features are visible as expected, corresponding to the two non-equivalent nitrogens of the porphyrins: the iminic nitrogen (–NH–) at high binding energies and the pyrrolic nitrogen (=N–) at low binding energies.[17,18] At intermediate θ_{Na} values, two different contributions are visible in both components; at $\theta_{Na} = 1.5$ the pristine components are not visible any longer.

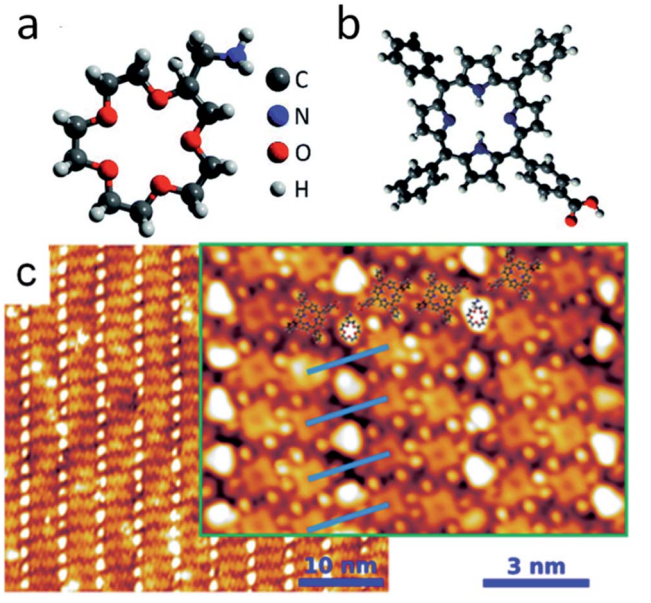

Fig. 1 3D graphic representation (geometry not optimized) of the AMC (a) and CTPP (b) molecules; (c) STM image of the 2D AMC array (1 × 2 phase) anchored on the CTPP template. STM image parameters: $V = -0.2$ V, $I = 0.2$ nA (inset: $V = -0.2$ V, $I = 1.0$ nA). Adapted from ref. 16.

The porphyrin doping is revealed also by the STM image shown in Fig. 2, where molecules with two different degrees of brightness are visible. The darker molecules are in their pristine state while the light ones have trapped one Na atom. By means of STM pulse manipulation experiments, we further investigated the properties of the doped CTPP and in particular we verified (i) the possibility to remove the Na atoms and recover the pristine appearance of CTPP molecules, as well as (ii) the existence of different conformations of the doped molecules (see ESI†). Some brighter spots are also visible in Fig. 2 (light blue circle) and may be either molecules possibly interacting with more than one Na, second layer molecules or molecules in a different geometric conformation. Even if falling out the scope of this work, we remark that both the STM and the XPS spectra indicate that the Na doping process of CTPP is not a spatially averaged interface effect: the Au–Na–CTPP interaction has a local character, giving (i) different appearance to the doped molecules and (ii) novel XPS components, which are observed in coexistence with the pristine (undoped) ones at the intermediate coverages. A molecular approach to the doping was already suggested for potassium doped phthalocyanines[19,20] in thicker layers. As was explained in that case, an electron from the alkali metal is delocalized on the hosting molecule with partial filling of the LUMO and the consequent lowering of the other electronic states with respect to the Fermi level. We can state here that the Na doping affects the film molecules locally, also with the possible mediation of the substrate, and that the chemical shift of XPS peaks cannot be merely ascribed to a spatially averaged modification of the organo-metallic interface. The effect of Na doping changes significantly, when dosing Na atoms on the array formed by AMC molecules anchored to the CTPP template.

In Fig. 3, we show the C 1s, N 1s and O 1s XPS spectra measured at different θ_{Na}. First of all, looking at the $\theta_{Na} = 0$ spectra (dark green curves), it has to be noticed that the different contributions from AMC and CTPP molecules can be easily discriminated. This is more evident for C 1s, where two well distinct peaks at ~286 and at ~284 eV are present, due to the AMC and CTPP respectively. In N 1s, a broad peak at ~401 eV is visible in addition to the two CTPP ones, which can be attributed to the amine termination of AMC involved in the amino-carboxylic anchoring.[21] The intensity ratio between this component and the CTPP ones, taking in consideration the number of N atoms present in the two molecules, gives a AMC : CTPP population ratio of 1 : 1.7, indicating that most of the surface (~86%) is covered by the 1 : 2 phase. The FWHM of

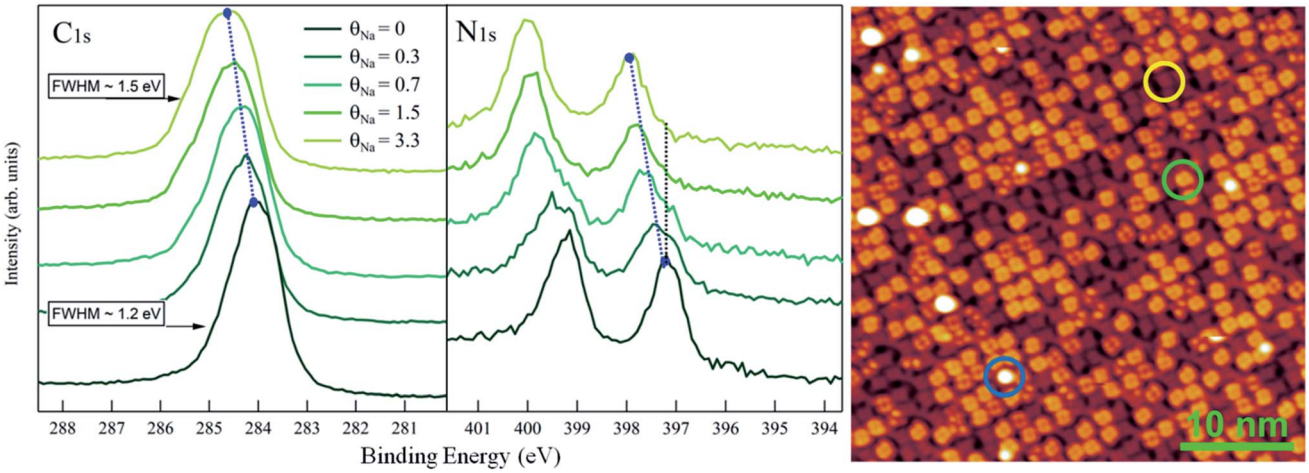

Fig. 2 Na deposition on the CTPP template. The doping effect of the alkali atoms is revealed by XPS as a shift towards the higher binding energies of both C 1s and N 1s peak (blue dashed lines). In N 1s, at intermediate Na coverages, two components can be distinguished, corresponding to the doped molecules and to the residual undoped ones (black dashed line). On the right panel, STM image taken at an intermediate θ_{Na}, shows undoped and doped and highly doped molecules as features with increasing level of brightness and indicated by yellow and green and blue circles respectively. Few bright spots (blue circles) are present whose nature is unclear. STM image parameters: $V = +1.0$ V, $I = 0.2$ nA.

the AMC component is 1.2 eV, much larger than the CTPP ones (~0.7 eV) possibly due to different configurations of the amino-carboxylic recognition scheme. This is in agreement with previously observed N 1s contribution of molecules involved in the same interaction.[21,22] Finally, the O 1s spectrum is dominated by the AMC contribution corresponding to a broad peak at ~532.2 eV. A shoulder at lower energies (~531.5 eV) is also recognizable and can be attributed to the carboxylic centers of the CTPP template hosting the amines of AMC.[21] Remarkably, the first stages of Na deposition, $\theta_{Na} = 0.5$ and $\theta_{Na} = 0.8$, only affect the photoemission features related to the AMC molecule, *i.e.* the main O 1s peak and the high binding energy C 1s component, both exhibiting a significant shift towards higher energies. The shifting of the CTPP C 1s and N 1s components starts only at $\theta_{Na} = 2.5$, where apparently the AMC peaks have reached a steady position. These findings support a description of the Na landing process where the alkali atoms at the beginning are trapped by the crowns and, only after saturation of the ether sites, start doping the underlying CTPP template. Interestingly, the N 1s and C 1s binding energy values of the doped CTPP molecules in the hetero-molecular layer (upper curves in Fig. 3), are higher than the corresponding values of the doped CTPP template reported in Fig. 2. The presence of the crown ethers, coordinated with Na atoms, affects the doping mechanism of the underlying CTPP molecules, making it apparently more effective. A clear explanation of this effect is missing and

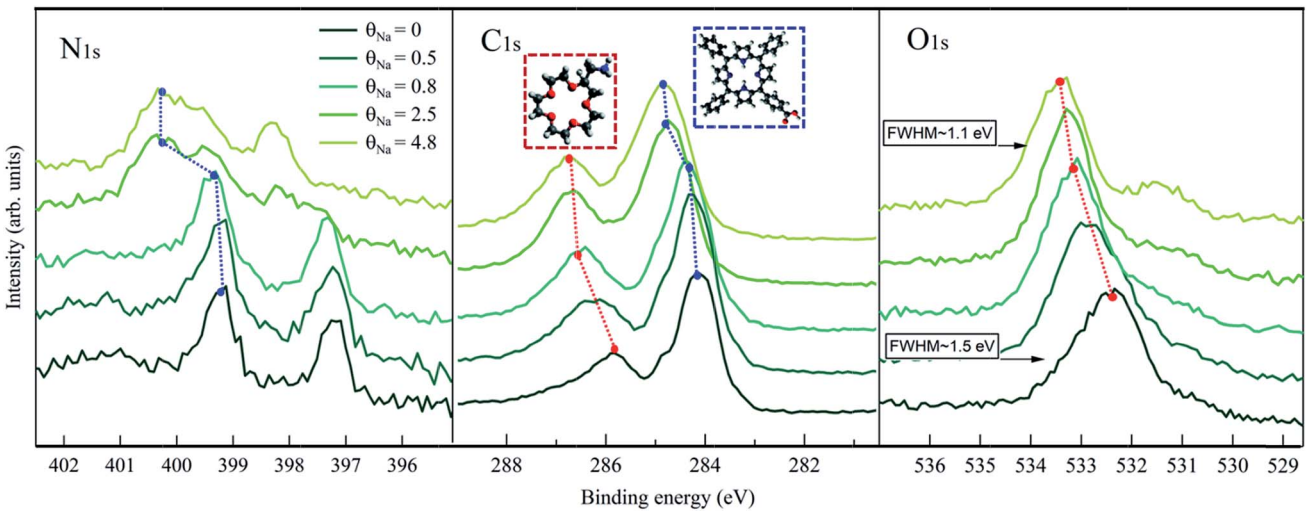

Fig. 3 XPS spectra on C 1s, N 1s and O 1s regions, taken at different Na coverage, θ_{Na}. The AMC related features are affected by the Na dosing at the early stages of deposition (red lines). On the contrary, a shift of CTPP peaks is evidenced only at higher θ_{Na} values (blue lines). This evidence supports the higher affinity of Na for AMC with respect to CTPP.

requires further investigation. The preferential trapping by the AMC molecules, is also consistent with the behavior of the Na 2p photoemission peak, shown in Fig. 4, where we identify two regimes. In the initial stages of doping we observe a single Na component at 30.25 eV, whose intensity is saturated at $\theta_{Na} = 0.8$. At higher Na coverage a new Na 2p component appears at ~0.2 eV higher binding energy, whose intensity increases linearly with coverage.

The STM image of a representative Na-doped interface is reported in Fig. 5. The first consideration to be done is that the array ordering of the guest crown molecules has been preserved, *i.e.* the presence of Na atoms does not affect the amino-carboxylic recognition. If compared with the STM image of Fig. 1, it is evident that the appearance of the crown molecules has changed, now resulting more *bean*-shaped rather than *round*-shaped. Moreover, even if a precise determination of θ_{Na} was not possible in the STM setup, we notice that while all the crown molecules have a different aspect with respect to the undoped systems, some CTPP molecules still display their pristine intramolecular contrast. This again supports preferential trapping of Na atoms by the ethers. In conclusion, we demonstrated the complexing functionality of an array of crown ethers anchored on a CTPP template, with the process being entirely obtained under UHV, from the crown template formation to the alkali metal deposition and trapping. This result opens on one hand to the possibility of exploiting crown derivatives in the on-surface formation of organo-metallic complex interfaces; on the other hand to the viability to monitor and characterize a process, the ion-crown complexation, which plays an important role in many biology- and medical-related processes.

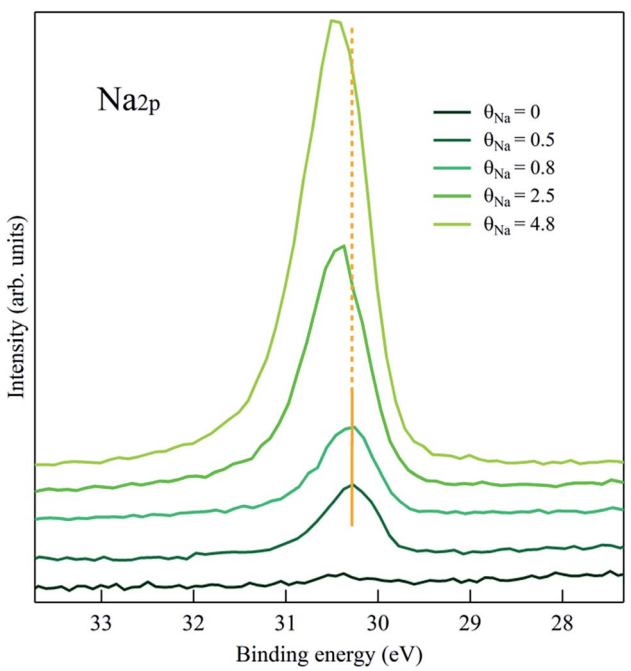

Fig. 4 Na 2p XPS on the Na/crown/CTPP system. According to what observed in Fig. 3, the second component at higher binding energy appears when also the CTPP template starts to be reached by the alkali atoms.

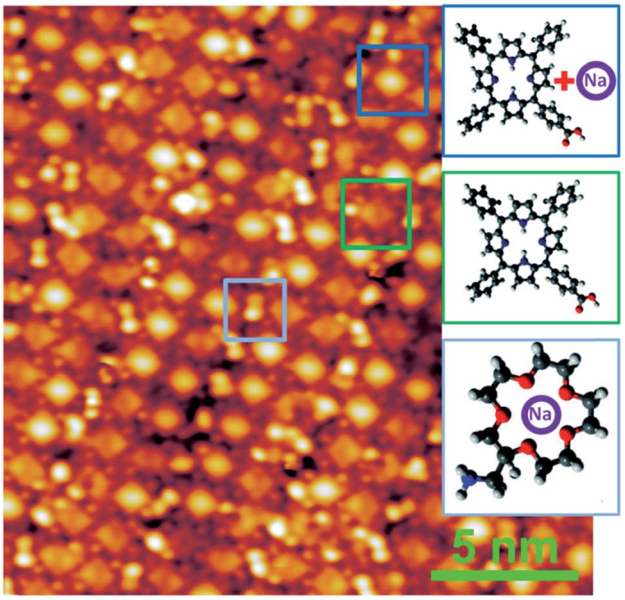

Fig. 5 STM imaging of the crown array upon Na trapping. The shape of the crown ethers has changed with respect to the pristine one shown in Fig. 1. Part of the underlying CTPP have still their undoped aspect. STM image parameters: $V = +0.1$ V, $I = 0.3$ nA.

Materials and methods

The AMC/CTTP interface has been prepared following the protocol described elsewhere.[16] Na atoms have been evaporated from a SAES alkali metal dispenser. The XPS measurements were performed at the ALOISA beamline[23] at the Elettra Synchrotron in Trieste, Italy. The C 1s and N 1s spectra have been taken with a photon of 500 eV of energy and overall resolution of 200 meV; the O 1s with a 650 eV photon energy and overall resolution of 250 meV; the Na 2p with 150 eV and overall resolution of 200 meV. The binding energy scale of the spectra has been determined by measuring the Au $4f_{7/2}$ peak as reference.[24] The sodium coverage θ_{Na} was determined by measuring the integrated intensity of Na 2p photoemission peak at binding energy of ~30 eV. As described in the text, the calibration of θ_{Na} was obtained after a deposition of the alkali metal on the bare Au(111) surface and the evaluation of the ratio between Na 2p intensity and the Au 4f surface component of the clean surface. The CTPP density for θ_{Na} definition was then estimated from the STM images of the CTPP template presented in ref. 16. STM imaging was performed with an Omicron Low-Temperature STM, hosted in a custom-built experimental UHV system at TASC Laboratory in Trieste, operating at a base pressure of 1×10^{-10} mbar. Electrochemically etched tungsten tips were used for imaging. Images were acquired in the constant current mode, at a temperature of approximately 5 K, and the bias reported in the images is the sample bias with respect to the tip (at ground); *i.e.*, a positive bias indicates imaging of the empty states of the sample.

Conflicts of interest

There are no conflicts to declare.

Notes and references

1 C. J. Pedersen, *J. Am. Chem. Soc.*, 1967, **89**, 2495–2496.
2 C. J. Pedersen, *J. Am. Chem. Soc.*, 1967, **89**, 7017–7036.
3 G. W. Gokel, W. M. Leevy and M. E. Weber, *Chem. Rev.*, 2004, **104**, 2723–2750.
4 M. B. More, D. Ray and P. B. Armentrout, *J. Am. Chem. Soc.*, 1999, **121**, 417–423.
5 S. Maleknia and J. Brodbelt, *J. Am. Chem. Soc.*, 1993, **115**, 2837–2843.
6 B. L. Williamson and C. S. Creaser, *Int. J. Mass Spectrom.*, 1999, **188**, 53–61.
7 R. Kusaka, S. Kokubu, Y. Inokuchi, T. Haino and T. Ebata, *Phys. Chem. Chem. Phys.*, 2011, **13**, 6827.
8 D. N. Reinhoudt, A. M. Eendebak, W. F. Nijenhuis, W. Verboom, M. Kloosterman and H. E. Schoemakerb, *J. Chem. Soc., Chem. Commun.*, 1989, 399–400.
9 D.-J. van Unen, J. F. J. Engbersen and D. N. Reinhoudt, *Biotechnol. Bioeng.*, 2002, **77**, 248–255.
10 J. Broos, I. K. Sakodinskaya, J. F. J. Engbersen, W. Verboom and D. N. Reinhoudt, *Chem. Commun.*, 1995, 255–256.
11 M. Kralj, L. Tušek-Božić and L. Frkanec, *ChemMedChem*, 2008, **3**, 1478–1492.
12 D.-W. Lim, S. A. Chyun and M. P. Suh, *Angew. Chem., Int. Ed.*, 2014, **53**, 7819–7822.
13 S. Yoshimoto, K. Suto, K. Itaya and N. Kobayashi, *Chem. Commun.*, 2003, **3**, 2174–2175.
14 S. Flink, F. C. J. M. Van Veggel and D. N. Reinhoudt, *J. Phys. Chem. B*, 1999, **103**, 6515–6520.
15 Y. Inokuchi, T. Ebata, T. Ikeda, T. Haino, T. Kimura, H. Guo and Y. Furutani, *New J. Chem.*, 2015, **39**, 8673–8680.
16 Z. Feng, G. Kladnik, G. Comelli, C. Dri and A. Cossaro, *Nanoscale*, 2018, **10**, 2067–2072.
17 J. M. Gottfried, K. Flechtner, A. Kretschmann, T. Lukasczyk and H. P. Steinrück, *J. Am. Chem. Soc.*, 2006, **128**, 5644–5645.
18 G. Lovat, D. Forrer, M. Abadia, M. Dominguez, M. Casarin, C. Rogero, A. Vittadini and L. Floreano, *Phys. Chem. Chem. Phys.*, 2015, **17**, 30119–30124.
19 T. Schwieger, H. Peisert, M. S. Golden, M. Knupfer and J. Fink, *Phys. Rev. B: Condens. Matter Mater. Phys.*, 2002, **66**, 155207.
20 A. Calabrese, L. Floreano, A. Verdini, C. Mariani and M. G. Betti, *Phys. Rev. B: Condens. Matter Mater. Phys.*, 2009, **79**, 115446.
21 A. Cossaro, M. Puppin, D. Cvetko, G. Kladnik, A. Verdini, M. Coreno, M. De Simone, L. Floreano and A. Morgante, *J. Phys. Chem. Lett.*, 2011, **2**, 3124–3129.
22 Z. Feng, C. Castellarin Cudia, L. Floreano, A. Morgante, G. Comelli, C. Dri and A. Cossaro, *Chem. Commun.*, 2015, **51**, 5739–5742.
23 L. Floreano, A. Cossaro, R. Gotter, A. Verdini, G. Bavdek, F. Evangelista, A. Ruocco, A. Morgante and D. Cvetko, *J. Phys. Chem. C*, 2008, **112**, 10794–10802.
24 A. Cossaro, L. Floreano, A. Verdini, L. Casalis and A. Morgante, *Phys. Rev. Lett.*, 2009, **103**, 119601.